Hindawi
Journal of Sensors
Volume 2022, Article ID 7049248, 9 pages
https://doi.org/10.1155/2022/7049248

Research Article

Microwave-Based Electrochemical Sensor Design by SRR Approach for ISM Sensing Applications

Vedat Özkaner,[1] Liton Chandra Paul,[2] Muharrem Karaaslan,[1] and Volkan Akdoğan[1]

[1]*Electrical and Electronics Engineering, Iskenderun Technical University, Hatay 31200, Turkey*
[2]*Electrical, Electronic and Communication Engineering, Pabna University of Science and Technology, Pabna 6600, Bangladesh*

Correspondence should be addressed to Liton Chandra Paul; litonpaulete@gmail.com

Received 15 September 2022; Revised 17 December 2022; Accepted 19 December 2022; Published 31 December 2022

Academic Editor: Kathiravan Srinivasan

This paper presents a transmission line and a split ring resonator (SRR) based sensor structure with a high sensitivity capacity to discriminate various methanol mixtures. The height of the dielectric layer and thickness of copper are assigned as 1.6 mm and 0.035 mm, respectively. The overall dimensions of the sensor structure are defined as 16 mm × 16 mm × 1.6 mm. The operating frequency is selected for the ISM bands, especially around 2.45 GHz. Different methanol-water mixtures are prepared at various ratios, and then, the complex permittivity values are measured. Different sensor structures are modelled and investigated using a two-port transmission line approach. Various types of SRR based sensors are designed, and an optimum design is proposed for methanol mixture detection applications. The observed quality factor of the proposed sensor is 16.5. The resonance shifts of the transmission value (S_{21}) are used for sensing capability around 2.45 GHz at -45 dB and 90 MHz resonance shifts. The sensitivity of the sensor has been evaluated as 1 MHz. Finally, the electric field distributions of the proposed SRR integrated transmission line are investigated. The novelty of the proposed design is to exactly sense the ratio of methanol in water with a very simple design. The proposed sensor structure can be used for methanol detection applications in medical, military, and chemical research.

1. Introduction

In the recent era, microwave sensing approaches are mainly used for various purposes such as moisture tissue detection [1, 2], oil quality control [3], humidity sensing, breast cancer detection [4], brain stroke detection [5], organic vapour sensing, flow rate measurement, and acetone-ethanol-methanol concentration detection [6]. Microwave sensing systems have many advantages such as real-time, noninvasive, flexibility, and high adaptation rate for many applications [7]. In most applications, the microwave technique paves the way for nondestructive test opportunities to detect many materials [8, 9]. In the literature, there are many approaches to improve the sensing capability of any type of sensor structure, such as the metamaterial approach with split-ring resonator (SRR) layers [10–12].

The most important part of a sensor structure is the resonator layer in microwave approach. Since this layer is the sensing part and must have a high sensing capability in any application. For example, Ebrahimi et al. proposed a transmission line with LC characteristics to sense the differential permittivity at operating frequencies between 2 GHz and 3 GHz [13]. Similarly, an analytical model is developed and proposed for complex permittivity sensing. The resonator section of this model is a combination of microstrip lines in the designed transmission line [14]. Han et al. suggested a planar microwave sensor loaded with a complementary curved ring resonator (CCRR) structure. The purpose of the sensor is to measure the permittivity value of the substrate material in microwave circuits based on integrated waveguide structure. Four different substrate materials have been tested to demonstrate that the proposed CCRR structure successfully increases the electric field intensity in the measuring area. It has been observed that the sensor has a high sensitivity and accuracy [15]. In addition, Coromina et al. proposed a capacitive loaded slow wave transmission

line system that has capability to sense permittivity characteristics [16]. Furthermore, the real part of the permittivity characteristics of a liquid sample has been successfully measured by a dual-band SRR sensor. Zidane et al. proposed an SRR-based hypersensitive microwave sensor structure to sense the glucose concentration in water. The operating frequency of this study is chosen as 1.9 GHz [17].

Microwave sensors are also used in biomedical applications such as equol level determination by Loutchanwoot and Harnsoongnoen. This paper has proposed a compact and straightforward microwave sensor for the quick detection of a wide range of highly concentrated materials utilising a little volume of equol. The complementary split-ring resonator (CSRR) with the Peano fractal geometry-loaded microstrip line has served as the foundation for the sensor structure's design. The proposed sensor has been discovered to identify the sample type as well as the equol concentration range [18]. A planar microstrip SRR-based sensor with an active feedback loop has been designed in [19] for organic vapour sensing applications. Another polydimethylsiloxane-(PDMS-) coated sensor has been proposed in [20] for detection of acetone vapour.

Moreover, studies on metamaterial-based liquid sensors [21], microfluidic sensors [22, 23], and oil sensors [24] have been integrated into the transmission line. Bhatti et al. determined the quality factor and sensitivity values for several oil samples. According to their findings, the suggested inexpensive sensor can be utilized in real-world scenarios with high accuracy to characterise edible oils and identify adulteration [25]. Also, planar CSRR sensor structure has been suggested to analyse various transformer oil samples by Srivastava et al. The operating frequency has been selected as 2.94 GHz. The sensor has displayed a frequency shift from 135.5 MHz to 470.5 MHz as the oil degrading time has been extended. The results have attributed to the actual alteration of the device's resonance frequency, the effective alteration of the dielectric constant, and effective capacitance between the waveguide and ground plane [26].

Moreover, Vélez et al. have investigated a microwave microfluidic sensor for dielectric characterization of liquids [27]. Three different sensors have been presented for microfluidic application. They have been based on CSRR (1.7 GHz), extended gap SRR (1.9 GHz), and conventional circular SRR (3.6 GHz) [28]. Liu et al. have also proposed a microfluidic sensor. An on-chip wideband microwave interferometry sensor has been utilized by improved sensitivity for differential sensing applications. Interference and loading an electrically small discontinuity structure at the sensing region are the two technologies employed to create the sensor. Different concentrations of NaCl and KCl solutions in DI water have been applied via the inlet and outlet [29].

In addition, various sensor designs have been engineered to enhance the accuracy of sensing ability and ethanol-water and methanol-water concentrations. For instance, Song and Yan have chosen the zeroth-order resonance (ZOR) mode to concentrate resonant energy on the surface element. The suggested sensor has implemented ZOR based on the series component. ZOR has been built with the shorted circuit of the composite left/right-handed transmission line resonant unit. The proposed sensor has a high sensitivity and reliable performance due to the miniaturised design, since it enhances the fraction of the detecting surface in the overall structure [30]. Prakash and Gupta have proposed a new complementary split ring resonator based sensor to sense chemical concentrations. Increasing the capacitive gap widths leads to a better coupling of electromagnetic energy from the transmission line to the resonator. The large sensing bandwidth of 1320 MHz has been obtained and circular-shaped CSRR has been chosen to improve liquid flow in the application [31]. Also, Parvathi and Gupta have presented an ultrahigh sensitivity and dense step via electromagnetic band-gap-based sensor to measure the complicated permittivity of mixtures of distilled water and ethanol. The centre frequency has been reduced to 2.38 GHz by the high inductance of SV-EBG compared to the centre-located via EBG (CLV-EBG) and edge-located via EBG (ELV-EBG) [32].

2. Dielectric Measurements

In the first step of this study, complex dielectric constants for five different methanol scenarios have been investigated. Methanol-water combinations of 20%, 40%, 60%, 80%, and 100% have been prepared and measured by a dielectric probe kit in microwave laboratory. Real parts of the measured complex dielectric constants have been given in Figure 1 that covers the range of 1 GHz-5 GHz. As clearly shown in the figure, 100% methanol has an average dielectric constant of 21 at 3 GHz. Therefore, 80%, 60%, 40%, and 20% methanol-water combinations have dielectric constants of nearly 30, 43, 55, and 63, respectively. This phenomenon is due to the differences between the dielectric characteristics of methanol and water. Pure water has a dielectric constant of approximately 75, and methanol has a nearly 20 at 3 GHz. As a result of these differences, various dielectric characteristics can be utilized to detect the methanol ratio.

3. Sensor Designs

In this research study, the main purpose is to discriminate between different types of water-methanol combinations. As given in Figure 1, different methanol-water mixtures have different dielectric characteristics, and this behaviour paves the way for sensor design. In the design and analysis steps, a finite integration-based microwave simulation software has been used. The FR4 dielectric material has been selected as a substrate layer, and copper metal has been assigned for both the resonator and ground layers. The selected FR4 has 1.6 mm thickness and 4.3 dielectric constant. FR4 dielectric substrate has been chosen due to low price and low loss characteristic at the related frequency range as well as widespread utilisation.

In the first sensor design, a two-ring-combined transmission line has been designed as shown in Figure 2(a). The operating frequency band has been chosen between 5 and 6 GHz. From Figure 2(b), the transmission resonance frequency of the proposed structure is around 5.55 GHz, and the amplitude at this frequency value is -3 dB. The reflection resonance frequency of the same structure is

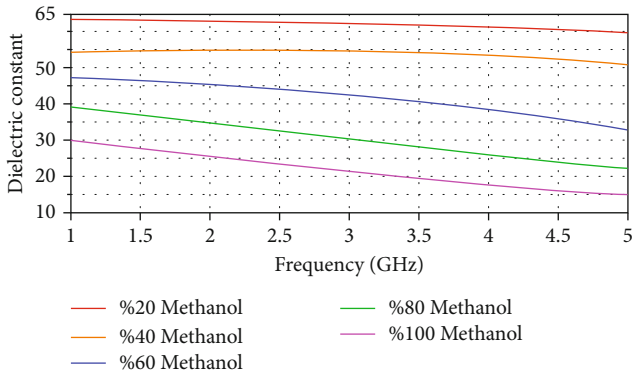

Figure 1: Measured dielectric constant values for 20%, 40%, 60%, 80%, and 100% methanol materials. The measurements are carried out by using a dielectric probe kit. The technique utilized in these measurements is an open-ended coaxial probe approach.

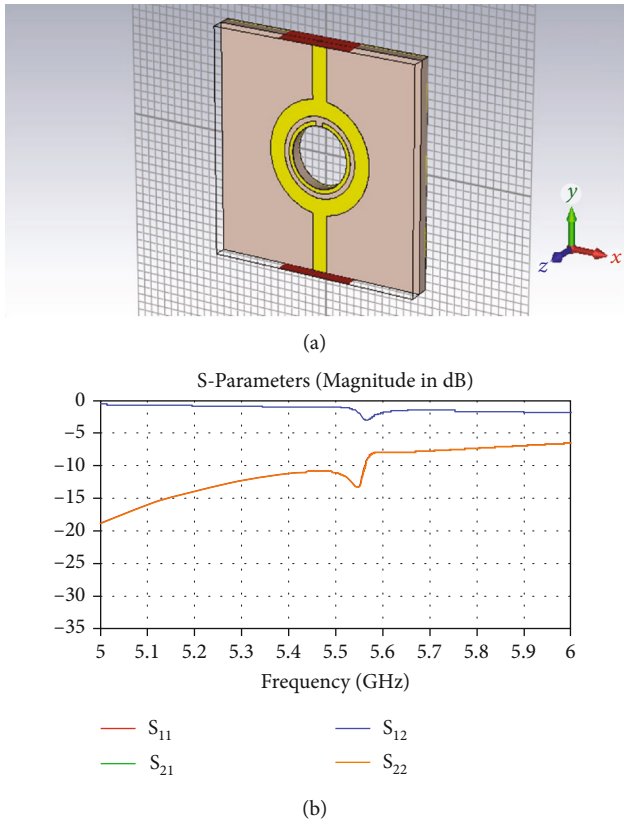

Figure 2: SRR-based 1st transmission line sensor design (a) and its scattering values (b).

5.53 GHz. The reflection coefficient of the structure at the frequency point is around -14 dB. As can be seen from Figure 2(b), nearly entire applied magnitude has been transmitted from the transmission line. Only a small resonance has been observed at 5.55 GHz. The inefficiency of the split-ring resonator placed in the ring is related with its much lower dimensions with respect to the ring. Since the transmission lines can be represented by lumped elements, the SRR can be represented by inductance and capacitance by ignoring resistance. The inductance and capacitance

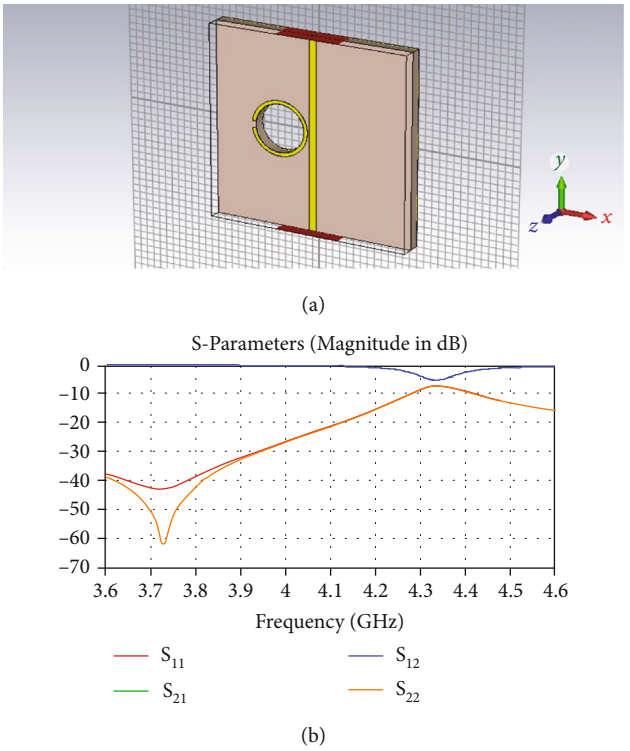

Figure 3: SRR-based 2nd transmission line sensor design (a) and its scattering values (b).

behave as LC resonator. These are created by mutual effect of the main outer ring. Since this mutual effect will be lower and the LC resonator will have a resonance at a single frequency, the transmission response only has a small resonance as demonstrated.

In the second sensor design, another two-port transmission line has been arranged, and the numerical results have been obtained. The split-ring resonator (SRR) and sensing gap have been located on the left side of the transmission line as illustrated in Figure 3(a). The aim of this sensing gap is to allow fluid flow and discriminate between sensing materials. In addition, the *S*-parameter characteristics of the second design are given in Figure 3(b). The structure has a transmission value of -6 dB at a frequency of 4.34 GHz. The differences in the resonance frequency and amplitude values of S_{11} and S_{22}, which are the reflection coefficients of the sensor structure, stem from the asymmetric structure of the structure. The S_{11} characteristic of the sensor structure is -43 dB at the resonant frequency of 3.73 GHz, and the S_{22} value is -62 dB at 3.74 GHz. As can be seen from Figure 3(b), applied wave has been transmitted exactly on the transmission line. A small resonance has been observed at 4.34 GHz. The inefficiency of the split-ring resonator placed to the left side of transmission line is related with its much lower mutual interaction with respect to the transmission line. The SRR placed outside can be represented by inductance and capacitance by ignoring resistance. The inductance and capacitance values of the SRR respond as LC resonator. These lumped responses are created by mutual effect of the wave propagating on transmission line.

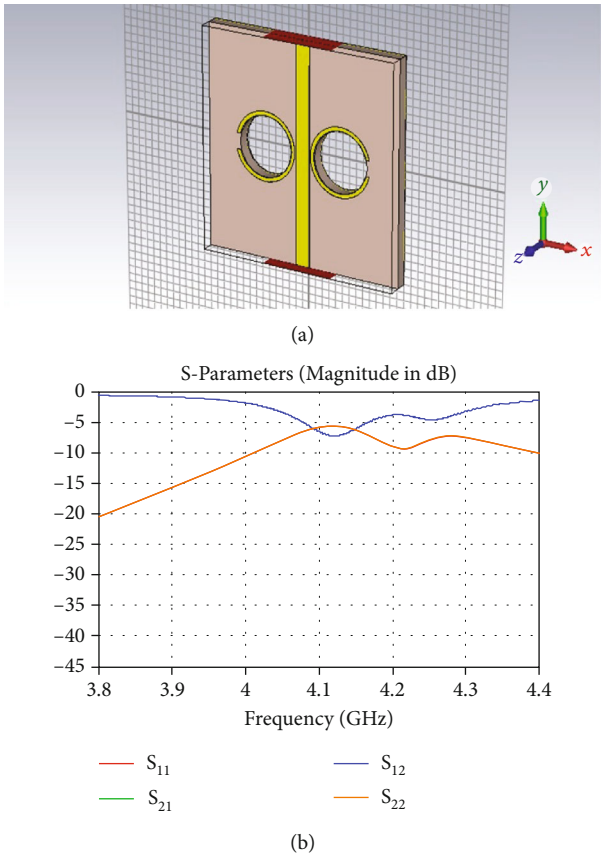

FIGURE 4: SRR-based 3rd transmission line sensor design (a) and its scattering values (b).

Since this mutual effect will be lower and the LC resonator will have a resonance at a single frequency, the transmission response only has a small resonance as demonstrated. The lower reflection and higher transmission with respect to the first design stem from the reduction of mutual interaction with the main carrier of EM wave, i.e., transmission line. The mutual interaction region between SRR and transmission line in the first design is much higher than the second one.

In the third design, a symmetric approach has been selected as shown in Figure 4(a). As clearly shown in Figure 4(b), the transmission and reflection values of the proposed structure are -7 dB and -9 dB at the resonance frequencies of 4.13 GHz and 4.22 GHz. As can be seen from Figure 4(b), applied wave has been transmitted with a high ratio on the transmission line. A resonance region has been observed at 4.13-4.22 GHz. The low effect of the split-ring resonators placed to both sides of transmission line is related with its lower mutual interaction with respect to the transmission line, but the mutual interaction is higher with respect to the second design, since this design includes two equivalent resonance SRRs. SRRs placed outside can be represented by inductance and capacitance by ignoring resistance. The inductance and capacitance values of the SRRs respond as two LC resonators parallel connected to main wave transmitter. These lumped responses are created by mutual effect of the wave propagating on transmission line.

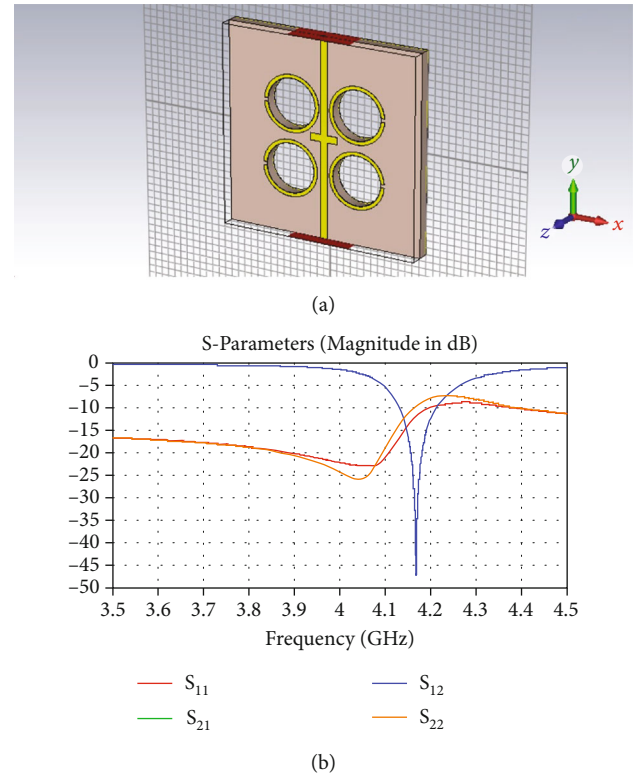

FIGURE 5: SRR-based 4th transmission line sensor design (a) and its scattering values (b).

Since this mutual effect will be low and the LC resonator will have a resonance at a frequency region due to two SRRs, the transmission response has low resonance as demonstrated. The higher reflection and lower transmission with respect to the second design stem from the increment of mutual interaction with the main carrier of EM wave, i.e., transmission line. This mutual interaction of the overall sensor system can be represented by a transmission line with an equivalent circuit composed of R-L-C-G and two parallel connected resonators that include L-C.

Furthermore, the fourth design proposes four sensing layers in the symmetric model as presented in Figure 5(a). However, the central metal patch causes different amplitudes in the reflections of each of the two ports, as shown in Figure 5(b). Although the reflection values of the proposed structure are not sufficient enough, the transmission values of the structure are at the desired level. The structure has a transmission value of -47 dB at a resonant frequency of 4.18 GHz. It can be seen from Figure 5(b) that applied wave from one port has been transmitted to one another with a high ratio on the transmission line at some part of the frequency range of 3.5-4.5 GHz. An exact resonance frequency region has been observed at around 4.18 GHz. The high effect of the split-ring resonators placed to both sides of the transmission line is related with its high mutual interaction with the transmission line at resonance frequency region. The mutual interaction is very high with respect to all the previous designs, since this design includes four equivalent resonance SRRs. SRRs placed at the left and right

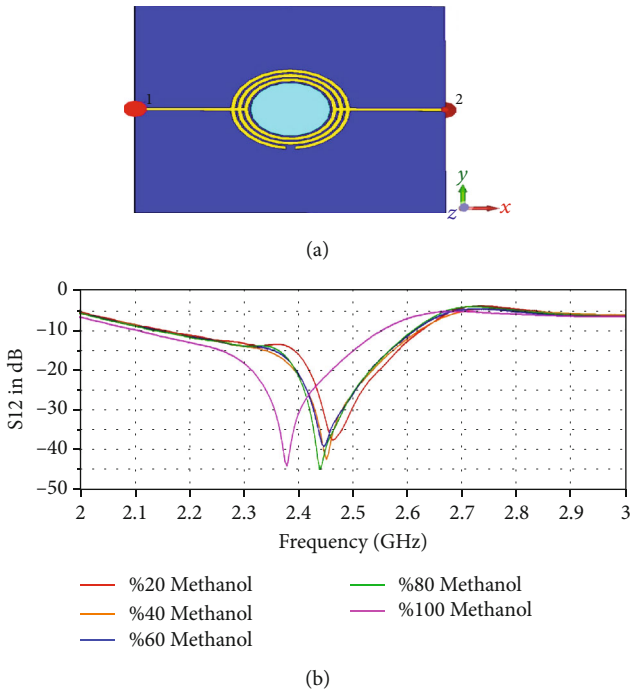

Figure 6: SRR-based proposed transmission line sensor design (a) and S_{12} results for 20%, 40%, 60%, 80%, and 100% methanol materials (b).

sides can be represented by inductance and capacitance. The inductance and capacitance values of the SRRs respond as four LC resonators parallel connected to main wave transmitter. These lumped responses are created by mutual effect of the wave propagating on the transmission line. Since this mutual effect will be high and the LC resonators demonstrate an exact resonance at a frequency region due to four SRRs, the transmission response has high resonance. The higher reflection and much lower transmission with respect to the previous designs result from the increment of mutual interaction with the main transmitter of EM wave, i.e., transmission line. Besides this, the cross line also contributes as an extra impedance on the transmission line.

4. Proposed Sensor Design and Results

Figure 6(a) shows the transmission line-based sensor structure designed to detect the methanol concentration. The structure consists of resonators with a thickness of 0.035 mm-nested circular rings. The outermost resonator has a 0.5 mm wide slit. In addition, the resonators have been placed on a 1.6 mm thick FR4-type substrate interface. The middle part of the structure has been excavated from the substrate interface, and a material sensing holder has been obtained. The TEM wavelength has been applied to the line by connecting a split port at both ends of the transmission line. The estimated dielectric constants have been defined for the material holder in Figure 6(b). As seen in the figure, the resonance frequencies for the samples with methanol concentrations of 20%, 40%, 60%, 80%, and 100% have been

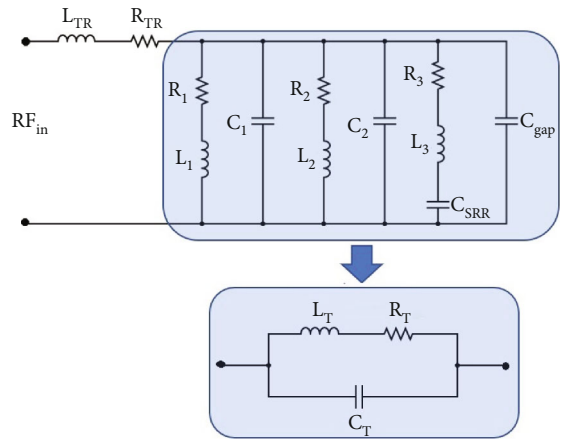

Figure 7: Equivalent circuit model of the proposed structure.

obtained as 2.47 GHz, 2.45 GHz, 2.44 GHz, 2.43 GHz, and 2.38 GHz, respectively. The total shift has been observed as 90 MHz. From this point of view, it has been seen that the designed sensor structure separates the different combinations of the methanol-water mixture.

The equivalent circuit model of the structure has been given in Figure 7. In this model, each nested circular loop must first consist of resistive (R1, R2, and R3) and inductive parts (L1, L2, and L3). After that, adjacent loops include shunt capacitances represented as $C1$ and $C2$. The outer loop has an extra capacitive element (CSRR) as it is designed as a split-ring resonator. The sample layer which is shown as the middle cylindrical area in the resonator acts as a capacitance (C_{gap}) in the equivalent circuit model shown in Figure 7. LTR and RTR represent the inductive and resistive parts of the transmission line. The overall model can be represented as LT, RT, and CT which are total inductance, resistance, and capacitance.

From the designed equivalent circuit model, it is considered that the only factor that can affect resonance frequency is CT.

$$C_T = C_{\text{adj}} + C_{\text{SRR}} + \varepsilon_{\text{samp}} C_{\text{gap}}. \tag{1}$$

C_{adj} is the total capacitance of the adjacent circular loops.

$$C_{\text{adj}} = C_1 + C_2. \tag{2}$$

When Equation (1) is examined, it can be found that the only part that can change the value of total capacitance (CT) is $\varepsilon_{samp} C_{gap}$. In this part, ε_{samp} represents the dielectric characteristic of the sample placed in the sensor layer, and it can be written as

$$\varepsilon_{\text{samp}} = \varepsilon'_{\text{samp}} + j\varepsilon''_{\text{samp}}. \tag{3}$$

Hence, the real and imaginary part of the sample permittivity (ε_{samp}) determines the overall value of the total

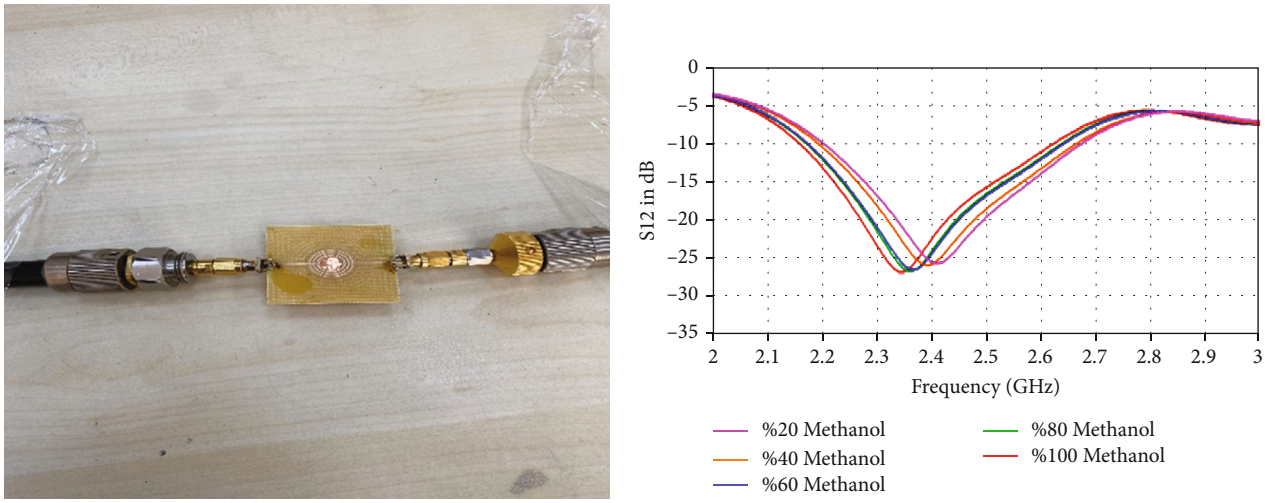

(a) (b)

Figure 8: Fabricated SRR-based proposed transmission line sensor design (a) and S_{12} results for 20%, 40%, 60%, 80%, and 100% methanol materials (b).

Table 1: Comparison of the simulation and measurement results at resonance frequencies for each percentage of methanol.

Sample ratio	Resonance frequency		S_{12} in dB	
	Simulation	Measurement	Simulation	Measurement
20% methanol	2.47 GHz	2.43 GHz	-37 dB	-25.5 dB
40% methanol	2.45 GHz	2.40 GHz	-42 dB	-25.7 dB
60% methanol	2.44 GHz	2.38 GHz	-39 dB	-26 dB
80% methanol	2.43 GHz	2.36 GHz	-45 dB	-26 dB
100% methanol	2.38 GHz	2.35 GHz	-44 dB	-26.5 dB

capacitance in the sensor structure. The total capacitance can be expressed as a function of sample permittivity.

$$C_T = F_T\left(\varepsilon'_{\text{samp}}, \varepsilon''_{\text{samp}}\right). \quad (4)$$

The resonance frequency which is calculated from the equivalent circuit model can be written as follows:

$$f_0 = \frac{1}{2\pi\sqrt{L_T C_T}}. \quad (5)$$

So any changes which stem from the sample characteristics in the sensor layer result in resonance frequency shift.

The fifth design has also been fabricated by using LPKF ProtoMat. All the dimensions and substrate are selected the same with the simulated sensor design. The measurements have been carried out between 2-3 GHz by using Agilent VNA. Two inputs of the VNA have been connected to both ports of the designed sensor. The liquid samples with various ratios of methanol have been placed in the hole in rings. The measurement results have been given in Figure 8. The resonances are around 2.35 and 2.43 GHz. The resonance frequency shifts to downward with the increment of methanol ratio. Hence, it can be emphasized that the simulation and measurement results are in good agreement.

The simulation and measurement results of the sensor structure in resonance frequencies have been tabulated as can be seen in Table 1. A small frequency shift with a maximum value of 80 MHz has been observed between measurements and simulations, but the frequency change for 20% methanol and 100% methanol cases are 90 MHz and 80 MHz for simulation and measurement results, respectively. The frequency and transmission value (S_{21}) differences stem from the fabrication errors of sensor, calibration errors, connection port losses, and cables losses.

Besides, the real part of dielectric constant of water is around 80 for the related frequency range. It means that its dielectric constant is the highest with respect to the waters including methanol. Adding the methanol to water decreases the dielectric constant of the sample under test as can be seen in Figure 1. The increment of the ethanol ratio in water results in frequency shift to downward. Hence, the transmission value (S_{21}) of pure water has been expected to resonate at the highest frequency at around 2.5 GHz. The electric field distribution of the proposed sensor has been given in Figure 9. First of all, the transmission coefficient of the material has been obtained by filling the sample holder part with air. In the figure, the resonance frequency is approximately 4 GHz and the transmission coefficient is 0.3 in magnitude.

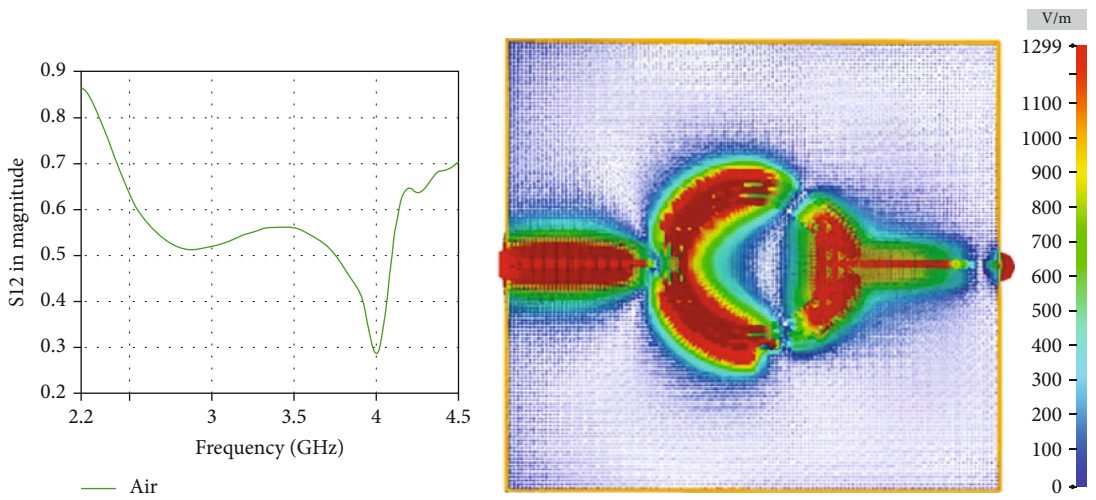

(a) (b)

Figure 9: *S*-parameter characteristics (a) and electric field distributions of the proposed SRR-based transmission line sensor (b).

Table 2: Response comparison of the designed sensors.

Sensor design	Resonance frequency	Resonance magnitude	Resonance shift	*Q* factor	Hall number
1	5.55 GHz	-3 dB	Not considered	—	1
2	4.34 GHz	-6 dB	Not considered	—	1
3	4.13 GHz	-7 dB	Not considered	—	2
4	4.18 GHz	-47 dB	20 MHz	209	4
5	2.45 GHz	-45 dB	90 MHz	16.5	1

Table 3: Comparison with previous works.

Study	Frequency (GHz)	Bandwidth (-10 dB)	Resonance frequency shift	Size (mm^3)	Resonator type
[25]	5.25	180 MHz	200 MHz	$30 \times 35 \times 1.6$	CSRR
[33]	2.325	150 MHz	50 MHz	$28 \times 20 \times 0.75$	CSRR
[34]	10	1.5 GHz	200 MHz	$22.86 \times 10.16 \times 1.6$	Metamaterial
[35]	10.5	120 MHz	60 MHz	$10 \times 10 \times 3$	Asymmetric electric SRR
This study	2.45	480 MHz	90 MHz	$16 \times 16 \times 1.6$	SRR

It is seen that a small portion of the energy transmitted from port 1 reaches to port 2. This proves the magnitude of the transmission coefficient shown in the figure. In addition to these, it has been seen that the electric field has generally concentrated on the resonators. The electric field distribution of the structure has been depicted for the resonance frequency of 4 GHz. The electric field component of the applied electromagnetic wave has been transmitted towards the ring with a high ratio. The electric fields have localised around the SRR, especially at the left part of the SRR. The right part of the SRR also resonates with the left part, and localization of electric fields has been observed at the right part, but the flow of the electric field decreased towards the next port (right side). Hence, the transmission of power also reduces at the same frequency value.

The responses of each sensor have been demonstrated in Table 2. Table 2 includes resonance frequency, resonance magnitude of transmission, bandwidth, *Q* factor, and number of halls in the sensor design. Since the resonance magnitude of transmission has been considered over -10 dB, the first three sensor designs have not been considered for methanol detection. The fourth and fifth sensor designs have sufficient transmission magnitudes with values of -47 dB and -35 dB at resonance frequencies, respectively. Whereas the *Q* factor of the fourth sensor design is very high with respect to the fifth design, the fifth sensor design has been selected to detect methanol ratio in water due to having only one hall.

The comparison of the proposed sensor with the studies in literature has been depicted in Table 3. Dielectric characterization of liquids has been realised by using microwave

sensor composed of CSRR in [33]. The resonance frequency of the designed sensor is around 2.325 GHz with a bandwidth of 150 MHz. The resonance shift has been observed around 50 MHz. Although the fabrication cost is low, the sensitivity and bandwidth are below the proposed design in this study. Liquid chemical detection has been also studied by using a metamaterial-based sensor [34]. In the study, the resonance frequency, bandwidth, and resonance shift have been shown at 10 GHz, 1.5 GHz, and 200 MHz, respectively. The drawback of this study is very high resonance frequency which can be affected by any circumference changes and results in abnormal shifts. Characterization and adulteration detection in edible oil has been performed by using microwave sensor [25]. In the study, the resonance frequency, bandwidth, and resonance shift are 5.25 GHz, 180 MHz, and 200 MHz, respectively. The fabrication process is based on PCB milling. The size of the microwave sensor is 30 mm × 35 mm, whereas the resonance shift of the sensor is higher. But the bandwidth is around 1/3 with respect to the designed sensor in our study. The sensing of liquids with low permittivity has been also carried out by utilising metamaterial-inspired microfluidic sensor [35]. The sensor dimension is extremely low (10 mm × 10 mm). The resonance frequency has been selected as 10.5 GHz. The disadvantage of the sensor is higher cost, low bandwidth (120 MHz), and low resonance shift (60 MHz). According to Table 3 and the characteristics of liquid sensors, the proposed sensor in our study is a good candidate to detect liquid characteristics in terms of dielectric constant change.

Hence, the strong sides of the proposed study can be summarized as it has the maximum bandwidth range/operating frequency ratio with respect to the other studies compared in Table 3. The selected frequency (2.45 GHz) is one of the most appropriate one due to the conventionally available range. The selected operating frequency in the study [33] is also similar with the proposed one, but the size of the sensing system in this study is lower than the sensor in [33]. Beside this, due to the higher wavelength, the proposed study will be affected less with respect to the studies [25, 34, 35].

5. Conclusions

In this study, a transmission line-based sensor to discriminate the methanol concentration in a mixture has been proposed. Four different SRR integrated transmission line sensors have been designed and investigated in the ISM bands. Afterwards, the final sensor structure has been developed with high resonance shift in transmission (S_{21}) characteristics at 2.45 GHz centre frequency. The dielectric constant values of water including various ratios of methanol have been determined in the frequency range of 1 GHz-5 GHz. It is observed that the dielectric constants are sufficiently different from each other to determine the ratio of methanol in water by designing a microwave sensor. The proposed sensor provides 480 MHz bandwidth, 90 MHz resonance frequency shift, small dimensions, and easy and cheap fabrication properties. Hence, the proposed sensor can be utilized to quickly quantify the amount of methanol in various fermented foods and drinks including alcohol.

Data Availability

The data used to support the findings of this study are included within the article.

Conflicts of Interest

The authors declare that they have no conflicts of interest.

References

[1] M. T. Jilani, M. Z. U. Rehman, A. M. Khan, O. Chughtai, M. A. Abbas, and M. T. Khan, "An implementation of IoT-based microwave sensing system for the evaluation of tissues moisture," *Microelectronics Journal*, vol. 88, pp. 117–127, 2019.

[2] S. Jiarasuwan, K. Chamnongthai, and N. Kittiamornkul, "A design method for a microwave-based moisture sensing system for granular materials in arbitrarily shaped containers," *IEEE Sensors Journal*, vol. 21, no. 17, pp. 19436–19452, 2021.

[3] A. E. Omer, S. Gigoyan, G. Shaker, and S. Safavi-Naeini, "Whispering-gallery-mode microwave sensing platform for oil quality control applications," *IEEE Internet of Things Journal*, vol. 9, no. 6, pp. 4065–4075, 2022.

[4] L. Wang, "Microwave sensors for breast cancer detection," *Sensors*, vol. 18, no. 2, p. 655, 2018.

[5] P. H. Tournier, M. Bonazzoli, V. Dolean et al., "Numerical modeling and high-speed parallel computing: new perspectives on tomographic microwave imaging for brain stroke detection and monitoring," *IEEE Antennas and Propagation Magazine*, vol. 59, no. 5, pp. 98–110, 2017.

[6] A. Rydosz, E. Maciak, K. Wincza, and S. Gruszczynski, "Microwave-based sensors with phthalocyanine films for acetone, ethanol and methanol detection," *Sensors and Actuators B: Chemical*, vol. 237, pp. 876–886, 2016.

[7] M. H. Zarifi and M. Daneshmand, "Liquid sensing in aquatic environment using high quality planar microwave resonator," *Sensors and Actuators B: Chemical*, vol. 225, pp. 517–521, 2016.

[8] Z. Li and Z. Meng, "A review of the radio frequency nondestructive testing for carbon-fibre composites," *Measurement Science Review*, vol. 16, no. 2, pp. 68–76, 2016.

[9] A. Wahab, M. M. A. Aziz, A. R. M. Sam, K. Y. You, A. Q. Bhatti, and K. A. Kassim, "Review on microwave nondestructive testing techniques and its applications in concrete technology," *Construction and Building Materials*, vol. 209, pp. 135–146, 2019.

[10] J. Mata-Contreras, C. Herrojo, and F. Martin, "Application of split ring resonator (SRR) loaded transmission lines to the design of angular displacement and velocity sensors for space applications," *IEEE Transactions on Microwave Theory and Techniques*, vol. 65, no. 11, pp. 4450–4460, 2017.

[11] S. Kiani, P. Rezaei, and M. Navaei, "Dual-sensing and dual-frequency microwave SRR sensor for liquid samples permittivity detection," *Measurement*, vol. 160, article 107805, 2020.

[12] K. T. Muhammed Shafi, M. A. Ansari, A. K. Jha, and M. J. Akhtar, "Design of SRR-based microwave sensor for characterization of magnetodielectric substrates," *IEEE Microwave and Wireless Components Letters*, vol. 27, no. 5, pp. 524–526, 2017.

[13] A. Ebrahimi, J. Scott, and K. Ghorbani, "Transmission lines terminated with LC resonators for differential permittivity

sensing," *IEEE Microwave and Wireless Components Letters*, vol. 28, no. 12, pp. 1149–1151, 2018.

[14] J. Muñoz-Enano, P. Velez, M. G. Barba, and F. Martín, "An analytical method to implement high-sensitivity transmission line differential sensors for dielectric constant measurements," *IEEE Sensors Journal*, vol. 20, no. 1, pp. 178–184, 2020.

[15] X. Han, X. Li, Y. Zhou et al., "Microwave sensor loaded with complementary curved ring resonator for material permittivity detection," *IEEE Sensors Journal*, vol. 22, no. 21, pp. 20456–20463, 2022.

[16] J. Coromina, J. Muñoz-Enano, P. Vélez et al., "Capacitively-loaded slow-wave transmission lines for sensitivity improvement in phase-variation permittivity sensors," in *2020 50th European Microwave Conference (EuMC)*, pp. 491–494, Utrecht, Netherlands, 2021.

[17] M. A. Zidane, A. Rouane, C. Hamouda, and H. Amar, "Hypersensitive microwave sensor based on split ring resonator (SRR) for glucose measurement in water," *Sensors and Actuators A: Physical*, vol. 321, article 112601, 2021.

[18] P. Loutchanwoot and S. Harnsoongnoen, "Microwave microfluidic sensor for detection of high equol concentrations in aqueous solution," *IEEE Transactions on Biomedical Circuits and Systems*, vol. 16, no. 2, pp. 244–251, 2022.

[19] M. H. Zarifi, M. Fayaz, J. Goldthorp, M. Abdolrazzaghi, Z. Hashisho, and M. Daneshmand, "Microbead-assisted high resolution microwave planar ring resonator for organic-vapor sensing," *Applied Physics Letters*, vol. 106, no. 6, article 062903, 2015.

[20] M. H. Zarifi, A. Sohrabi, P. M. Shaibani, M. Daneshmand, and T. Thundat, "Detection of volatile organic compounds using microwave sensors," *IEEE Sensors Journal*, vol. 15, no. 1, pp. 248–254, 2015.

[21] A. Tamer, F. O. Alkurt, O. Altintas et al., "Transmission line integrated metamaterial based liquid sensor," *Journal of the Electrochemical Society*, vol. 165, no. 7, pp. B251–B257, 2018.

[22] O. Altıntaş, M. Aksoy, E. Ünal, M. Karaaslan, and C. Sabah, "Operating frequency reconfiguration study for a split ring resonator based microfluidic sensor," *Journal of the Electrochemical Society*, vol. 167, no. 14, article 147512, 2020.

[23] A. Ebrahimi, J. Scott, and K. Ghorbani, "Ultrahigh-sensitivity microwave sensor for microfluidic complex permittivity measurement," *IEEE Transactions on Microwave Theory and Techniques*, vol. 67, no. 10, pp. 4269–4277, 2019.

[24] M. Erdoğan, E. Ünal, F. Ö. Alkurt, Y. I. Abdulkarim, L. Deng, and M. Karaaslan, "Determination of frying sunflower oil usage time for local potato samples by using microwave transmission line based sensors," *Measurement*, vol. 163, article 108040, 2020.

[25] M. H. Bhatti, M. A. Jabbar, M. A. Khan, and Y. Massoud, "Low-cost microwave sensor for characterization and adulteration detection in edible oil," *Applied Sciences*, vol. 12, no. 17, p. 8665, 2022.

[26] R. Srivastava, Y. Kumar, S. Banerjee, and S. N. Kale, "Real-time transformer oil monitoring using planar frequency-based sensor," *Sensors and Actuators A: Physical*, vol. 347, article 113892, 2022.

[27] P. Vélez, L. Su, K. Grenier, J. Mata-Contreras, D. Dubuc, and F. Martín, "Microwave microfluidic sensor based on a microstrip splitter/combiner configuration and split ring resonators (SRRs) for dielectric characterization of liquids," *IEEE Sensors Journal*, vol. 17, no. 20, pp. 6589–6598, 2017.

[28] N. Sharafadinzadeh, M. Abdolrazzaghi, and M. Daneshmand, "Investigation on planar microwave sensors with enhanced sensitivity from microfluidic integration," *Sensors and Actuators A: Physical*, vol. 301, article 111752, 2020.

[29] W. Liu, J. Zhang, and K. Huang, "Wideband microwave interferometry sensor with improved sensitivity for measuring minute variations in dielectric properties of chemical liquids in microfluidic channels," *Measurement*, vol. 189, article 110474, 2022.

[30] X. Song and S. Yan, "A sensitivity-enhanced sensor based on zeroth-order resonance for liquid characterization," *IEEE journal of electromagnetics, RF and Microwaves in Medicine and Biology*, vol. 6, no. 3, pp. 391–398, 2022.

[31] D. Prakash and N. Gupta, "High-sensitivity grooved CSRR-based sensor for liquid chemical characterization," *IEEE Sensors Journal*, vol. 22, no. 19, pp. 18463–18470, 2022.

[32] K. S. L. Parvathi and S. R. Gupta, "Ultrahigh-sensitivity and compact EBG-based microwave sensor for liquid characterization," *IEEE Sensors Letters*, vol. 6, no. 4, pp. 1–4, 2022.

[33] E. L. Chuma, Y. Iano, G. Fontgalland, and L. L. B. Roger, "Microwave sensor for liquid dielectric characterization based on metamaterial complementary split ring resonator," *IEEE Sensors Journal*, vol. 18, no. 24, pp. 9978–9983, 2018.

[34] Y. I. Abdulkarim, L. Deng, H. Luo et al., "Design and study of a metamaterial based sensor for the application of liquid chemicals detection," *Journal of Materials Research and Technology*, vol. 9, no. 5, pp. 10291–10304, 2020.

[35] Y. Cao, K. Chen, C. Ruan, and X. Zhang, "Robust and sensitive metamaterial-inspired microfluidic sensor for liquids with low dielectric constants," *Sensors and Actuators A: Physical*, vol. 331, article 112869, 2021.